Characterization of the Fast-Forming Intermediate, Des [30−75], in the Reductive Unfolding of Onconase†

Guoqiang Xu, Mahesh Narayan, Ervin Welker, and Harold A. Scheraga*

Baker Laboratory of Chemistry and Chemical Biology, Cornell University, Ithaca, New York 14853-1301

Received December 9, 2003; Revised Manuscript Received January 16, 2004

ABSTRACT: A fast-forming intermediate in the reductive unfolding of frog onconase (ONC), des [30−75], analogous to the des [40−95] intermediate found in the reductive unfolding of its structural homologue, bovine pancreatic ribonuclease A (RNase A), has been isolated and characterized. The midpoints of the thermal transition and chemical denaturing curves (representing *global* unfolding) indicate that the conformation of des [30−75] is considerably less stable than that of the parent molecule, suggesting that the (30−75) disulfide bond plays a significant role in the conformational stability of ONC. While des [30−75] is formed very quickly by a partial reduction of the parent molecule in a *local* unfolding step, it is not as easily susceptible to further reduction, indicating that its three disulfides are much more buried compared to the (30−75) disulfide bond in the parent protein. The nature of des [30−75] is similar to that of des [40−95] RNase A, in that des [30−75] ONC is also a disulfide-secure species. In addition, based on the resistance to mild reducing conditions, structured des species appear to form in ONC from unstructured three-disulfide-containing ensembles. This step is key in the oxidative folding of RNaseA, and is much faster in ONC than the formation of the structured des [40−95] species in RNase A.

Onconase (ONC)[1] is the smallest member of the bovine pancreatic ribonuclease A (RNase A) superfamily, with 104 amino acids compared to 124 in the defining member (*1*). These two proteins, ONC and RNase A, share about 30% identity in the amino acid sequences, and each has four disulfide bonds. The three-dimensional structure of ONC is very similar to that of RNase A, with major differences being present in the loop regions and at the C-terminus (*2*). An additional disulfide bond between Cys 87 and Cys 104 at the C-terminus of ONC replaces the (65−72) disulfide bond of RNase A. Notably, during the oxidative folding of RNase A, the (65−72) disulfide bond is favored over all other disulfide bonds because of its small loop size and favorable enthalpic interactions (*3*−*7*). Furthermore, the N-terminus in ONC has a pyroglutamic acid residue due to cyclization of Glu 1 (*1*), and its $O^{\epsilon 1}$ atom forms a hydrogen bond with Lys 9 N^{ζ} (*2*).

Although the two proteins have very similar three-dimensional structures, they demonstrate remarkable differences in stability, catalytic activity (affected by the hydrogen bonding described above), and toxicity (*8*−*13*). Close to neutral pH, the midpoint of the thermal transition of ONC is around 90 °C, which is ∼25 °C higher than that of RNase A (*8*−*13*). Ribonucleolysis experiments with ONC and RNase A, using two different ribonucleic acids as substrates, demonstrated that the ribonucleolytic activity of ONC is several hundred times less than that of RNase A (*1*, *14*, *15*). Furthermore, the [C87A, C104A] mutant of ONC, which lacks the (87−104) disulfide bond, has less cytotoxic activity than the native enzyme and has a significantly lower thermal transition (the midpoint of the thermal transition T_m is 60 °C), which demonstrates the substantial contribution of this synapomorphic disulfide bond to the toxicity and stability of the wild-type protein (*16*, *17*).

Ongoing work in our laboratory focuses on understanding the intramolecular interactions that govern the folding process of a polypeptide. We have used RNase A as a model system (*18*−*21*) for identifying the essential features of the oxidative folding process, in which the fully reduced polypeptide acquires its native disulfides and native structure. By characterizing the intermediates that are populated during the regeneration, we gain insight into the nature of the intramolecular interactions that direct the process along specific oxidative folding pathways (*22*−*24*).

The reverse of oxidative folding is reductive unfolding, during which proteins lose their three-dimensional structure (unfold) upon the reduction of their disulfides. Reductive unfolding can provide information about the nature of the

† This work was supported by the National Institute of General Medical Sciences of the National Institutes of Health (Grant No. GM-24893). Support was also received from the National Foundation for Cancer Research.

* To whom correspondence should be addressed: Tel. (607) 255-4034; fax (607) 254-4700; e-mail: has5@cornell.edu.

[1] Abbreviations: ONC, frog onconase (*Rana pipiens*); N-ONC, native onconase; R-ONC, reduced onconase; Ir, a three-disulfide-containing intermediate that is formed rapidly during the reductive unfolding of ONC; RNase A, bovine pancreatic ribonuclease A; *n*S, an ensemble of disulfide-containing intermediates each having *n* disulfide bonds; des [x−y], intermediate of RNase A or ONC having all native disulfide bonds but lacking the (x−y) disulfide bond; AEMTS, 2-amino ethylmethylthiosulfonate; DTT^{red} and DTT^{ox}, reduced and oxidized dithiothreitol, respectively; GdnHCl, guanidine hydrochloride; EDTA, ethylenediaminetetraacetic acid; Tris-HCl, tris(hydroxymethyl) aminomethane hydrochloride; HEPES, *N*-2-hydroxyethylpiperizine-*N*′-2-ethanesulfonic acid; HPLC, high performance liquid chromatography; UV, ultraviolet, ESI/FTMS, electrospray ionization/Fourier transformed mass spectrometry; MALDI-TOF, matrix-assisted laser desorption/ionization time-of-flight.

10.1021/bi036215d CCC: $27.50
Published on Web 02/27/2004

unfolding processes that are required for the exposure of the protein disulfides during the reduction of the native protein as well as its intermediates. It can be used as a probe for gathering information about the stability of the protein and its intermediates toward reduction. Furthermore, reductive unfolding is a useful tool to populate certain structured native disulfide-containing intermediates for further characterization that are critical in the oxidative folding and/or reductive unfolding process (*25*−*29*).

The single intermediate, des [30−75] ONC, arising from the partial reductive unfolding of ONC is of special interest in oxidative folding studies since it is analogous to des [40−95], the major structured intermediate formed in the oxidative folding of RNase A (*23*). In this work, we have characterized some physical and kinetic properties of des [30−75] ONC. By measuring the thermal transition and chemical denaturing curves of des [30−75] ONC, we have estimated the free energy of unfolding of this intermediate and obtained information about the contribution of this disulfide bond to the overall stability of the frog ribonuclease. We have also assessed the susceptibility of the disulfides of des [30−75] to further reduction, and have estimated the free energy of reduction of the intermediate.

Structured 3S intermediates that are known to play key roles in determining the regeneration pathways of RNase A were also detected in the oxidative folding of ONC (unpublished experiments). Since des [30−75] forms quantitatively from native ONC during its reductive unfolding, it is possible to isolate it in the unblocked form with a good yield, which, in turn, facilitates both the study of the kinetic fate of this species in oxidation and in the preparation of its unstructured 3S isomers. The unstructured, unblocked 3S isomers were used for determining the rate of the formation of the structured 3S species through reshuffling reactions. The relative abundance of the des species arising from reshuffling reactions is analyzed against a fully entropic model for all three-disulfide-bond-containing species and is compared with the same process in RNase A.

EXPERIMENTAL PROCEDURES

Materials. AEMTS (>99% pure) was purchased from Anatrace and used without further purification. DTT^{red} and DTT^{ox} were obtained from Sigma, and the latter was purified by reversed-phase HPLC. All other chemicals were of the highest grade commercially available. WT-onconase cDNA in a pet11 expression vector was kindly provided by R. J. Youle (*10*). The cDNA was amplified by PCR and cloned to a pet22b(+) vector in-frame with the pelB signal sequence without the starting methionine residue. WT-ONC was expressed in BL21 cells and purified as described elsewhere (*30*), and the level of expression was compared to that from another wild-type plasmid of ONC (pONC) which was kindly provided by R. T. Raines (*11*). Conversion of the N-terminal glutamine of the uncyclized residue to pyro-glutamic acid was carried out by dialyzing the folded protein against either 0.1 M HCl or 200 mM pH 7 phosphate buffer at room temperature for 2 days and checked by mass spectrometry. Recombinant ONC from our lab was found to coelute on an HPLC chromatogram with a test sample obtained from Dr. Youle.

Identification of the Fast-Forming Intermediate in the Reductive Unfolding of ONC. The methodology used to identify the nature of the reductive intermediate that appears during the reductive unfolding of ONC has been described in detail elsewhere (*30*). Briefly, the intermediate was isolated from N and R using a reversed-phase column, blocked with AEMTS and subjected to peptide mapping using proteolytic digestion and MALDI-TOF and also by ESI/FTMS. Analysis of the data from these two independent techniques revealed that the fast-forming intermediate lacked the (30−75) disulfide bond.

Isolation of Des [30−75]. Trial experiments demonstrated that the des [30−75] intermediate can be optimally populated 100 min after initiation of the reduction of ONC using 100 mM DTT^{red} at pH 8 (100 mM Tris-HCl and 1 mM EDTA) and 15 °C. A total of 1 mg of N-ONC (0.5 mg/mL) was subjected to such reducing conditions after which the sample was quenched by glacial acetic acid. Removal of buffer salts, DTT^{red}, and trace amounts of N-ONC was accomplished by semipreparative reversed-phase HPLC. Water and organic solvents were removed by lyophilization. The intermediate was used immediately after lyophilization and any unused material was stored at −80 °C to avoid air oxidation.

Determination of the Midpoint (T_m) of the Thermal Transition of Des [30−75]. The method for determining the thermal transition curve of the des species and its midpoint has been described previously (*31*). It is necessary to use this method because the UV absorbance yielded uninterpretable thermal denaturation curves because of precipitation, as observed in a previous study (*11*).

Determination of the Midpoint of the GdnHCl Denaturation of Des [30−75]. The same principle that was used previously (*31*) in obtaining the thermal transition curve for this reductive unfolding intermediate was applied to determine its chemical (GdnHCl) denaturing curve. Aliquots of des [30−75] (0.5 mg/mL in 1 mM acetic acid, pH 5) were dissolved separately into solutions of a 10 mM HEPES, 1 mM EDTA buffer (pH 7) that contained varying amounts of GdnHCl (0−6 M). The protein was allowed to equilibrate at 25 °C for 20 min in each denaturing solution. Then, a reduction-pulse (5 mM DTT^{red}, 2 min, final pH 8) was applied to reduce any conformationally unfolded or possibly reshuffled des [30−75] species. The reduction-pulse was followed by blocking all free thiols with an excess amount of AEMTS. After 5 min, the pH of the sample was reduced to 3 by adding glacial acetic acid and then the sample was desalted using a G25 column. Analysis of the desalted samples was carried out using cation-exchange HPLC (Rainin Hydropore 5-SCX column). The protein species were eluted from the column by application of a linear salt gradient (50−150 mM NaCl from 20 to 150 min). The fractional concentrations of des [30−75] and fully reduced ONC were obtained by integration of the well-separated peak areas corresponding to those two species. A control experiment for determining the GdnHCl denaturing curve of RNase A by this method was carried out.

It has to be noted that, in the method described above, the accessibility of the disulfide bonds is used to report on protein stability, and thus, in certain cases, the results may indicate local conformational changes that are not associated with the global unfolding/folding transition of the protein. Nevertheless, such limitations can also occur when using unevenly distributed optical probes within the protein, such as a single Tyr or Trp residue in an isolated domain of the

protein, which would then report only on local conformational changes. Also, strictly speaking, ours is not an equilibrium measurement, because the reduction of the unfolded population during the experiment may shift the equilibrium slightly (*31*). Nevertheless, as the RNase A experiment showed, it provides a reasonably good lower estimate for determining the midpoint of the unfolding transition (*31*).

Thermodynamic Parameters Estimated from Chemical Denaturation of Des [30−75]. For the analysis of the thermodynamic parameters, we have used a two-state model [this is the same model used for the chemical denaturation of native RNase A and native ONC under similar conditions (*9*, *10*, *12*, *13*)]. The free energy of conformational unfolding of a protein, ΔG^{o}_{cu} (cu: conformational unfolding), at different denaturant concentrations can be calculated by the following equation after obtaining the fraction of native protein by integrating the peak areas in the HPLC chromatogram.

$$\Delta G^{o}_{cu} = -RT \ln K_D = -RT \ln \frac{f_D}{f_N} \quad (1)$$

Here, K_D is the unfolding equilibrium constant; f_D and f_N are the fractions of denatured and folded species, respectively (i.e., f_N represents the fraction of native RNase A or des [30−75] ONC); R is the universal gas constant and T is absolute temperature. By linear extrapolation of the chemical denaturing curve in the range of a 0.95 to 0.05 fraction of native protein to zero denaturant concentration according to eq 2, the free energy of unfolding can be obtained at the experimental temperature (*32*−*34*). The free energy of unfolding (ΔG^{o}_{cu}) provides a measure of the stability of the protein under the given conditions.

$$\Delta G^{o}_{cu} = \Delta G^{o}_{cu}(H_2O) - mC_{GdnHCl} \quad (2)$$

Here, m is a measure of the dependence of the free energy on the denaturant, and C_{GdnHCl} is the concentration of GdnHCl. The extrapolation for des [30−75] was based on the data at concentrations of GdnHCl higher than 1.5 M (or 0.1 fraction of des [30−75]) because of nonlinearity at low concentrations, which was also observed in the GdnHCl denaturation of wild-type RNase A under certain conditions (*35*). This nonlinearity might be an indication of the deviation from a two-state mechanism (*35*).

Reductive Unfolding of Des [30−75]. Freshly obtained des [30−75] was dissolved into 200 μL of a pH 3 acetic acid solution (5 mg/mL protein concentration). DTT^{red} (30.8 mg) was dissolved by 1.8 mL of a buffer containing 20 mM Tris-HCl and 1 mM EDTA (pH 8) and incubated at 15 °C. Reductive unfolding was initiated by introducing 200 μL of solution containing des [30−75] into 1.8 mL of the pre-equilibrated buffer containing the reducing agent. The final concentration of DTT^{red} and des [30−75] ONC was 100 mM and 0.5 mg/mL, respectively. Aliquots of 200 μL were withdrawn at different times after the start of the reaction, and the free thiols in each aliquot were blocked by an excess amount of AEMTS. Five minutes after the addition of AEMTS, the pH of the samples was reduced to 3 by the addition of glacial acetic acid. The sample was desalted and analyzed by cation-exchange HPLC, as described in the previous subsection.

Oxidation of Des [30−75]. The oxidation of the des species was carried out by dissolving the lyophilized intermediate in 2 mL (0.5 mg/mL) of a 20 mM Tris-HCl, 1 mM EDTA buffer (pH 8), which contained DTT^{ox} (50 mM final concentration) and a small amount of DTT^{red} (0.4 mM final concentration) which had been incubated previously at 15 °C. The presence of a small amount of DTT^{red} is sufficient to reduce any unstructured intermediates that might form (giving rise to an indirect pathway) during the oxidation of des [30−75] to N-ONC (*36*). Aliquots of 200 μL of the reaction solution were periodically blocked by an excess amount of AEMTS and quenched by glacial acetic acid after a 5-min blocking time. The sample was desalted and analyzed by cationic-exchange HPLC.

Formation of Structured 3S Species from Its Unstructured 3S Ensembles. To produce the unstructured 3S isomers of des [30−75], the structured intermediate must first be allowed to reshuffle. Therefore, des [30−75] was dissolved into a 6 M GdnHCl buffer (pH 8, 100 mM Tris-HCl, 1 mM EDTA) and incubated for 1 h at 25 °C to achieve an equilibrium distribution of the 3S ensemble (final protein concentration of 0.5 mg/mL). The buffer had been sparged with argon prior to the addition of des [30−75], and argon sparging was continued during the course of the experiment. The sample was quenched by 20 μL of glacial acetic acid, and buffer salts and GdnHCl were removed by reversed-phased HPLC. Water and organic solvents were removed from the sample by lyophilization. That des [30−75] had been converted to its 3S isomers was confirmed by analyzing a small amount of the lyophilized sample by cation-exchange HPLC after AEMTS-blocking. In this chromatogram, des [30−75] elutes as a single sharp peak, whereas the unstructured 3S isomers elute over a broad retention time-interval with superposed multiple peaks.

The formation of structured three-disulfide-containing intermediates of ONC was initiated by adding 4 mL of a 20 mM Tris-HCl, 1 mM EDTA buffer (pH 8, 25 °C) to the lyophilized unstructured 3S ensemble [It should be noted that, in this experiment, a different temperature was used (25 °C) compared to that for characterizing des [30−75] elsewhere in this paper (15 °C)]. Aliquots of 0.5 mL samples were withdrawn at different times and subjected to a reduction pulse (3 mM DTT^{red}, 2 min) followed by AEMTS-blocking of all free thiols. The pH of the sample was reduced to 3 by the addition of glacial acetic acid. The sample was desalted and analyzed as described earlier. The application of a reduction pulse before blocking the samples reduces all unstructured 3S isomers to the fully reduced protein, which facilitates the separation of structured and unstructured 3S species in HPLC.

RESULTS

Midpoint of the Thermal Transition Curve (T_m). The midpoint of the thermal transition curve of the unblocked fast-forming intermediate, des [30−75], is 57.6 °C at pH 7 (*31*). This is slightly lower than both that of a mutant [C87A, C104A] ONC, which lacks the (87−104) disulfide bond (*15*), and that of wild-type RNase A (*9*, *37*, *38*). However, this value is much higher than that of a mutant of RNase A,

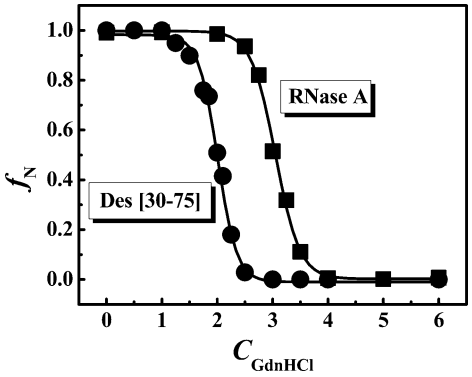

FIGURE 1: GdnHCl denaturing curves of des [30−75] ONC and RNase A at 25 °C and pH 7. The protein concentration is ~0.1 mg/mL.

Table 1: Thermodynamic Parameters of the GdnHCl-Induced Denaturation of ONC, Des [30−75] ONC, RNase A, and a Mutant [C40A, C95A] of RNase A at 25 °C

proteins	ΔG^o_{cu} (H_2O) (kcal mol^{-1})	$C_{1/2}$ (GdnHCl) (M)	m (kcal mol^{-1} M^{-1})
ONC[a]	13.9 ± 0.6	4.5	3.1 ± 0.2
des [30−75] ONC[b]	6.6 ± 0.7	2.0	3.3 ± 0.4
RNase A[b]	8.6 ± 0.4	3.0	2.8 ± 0.1
RNase A[c]	8.7 ± 0.2	3.0	2.9 ± 0.1
RNase A[d]	9.2 ± 0.6	3.0	3.1 ± 0.2
[C40A, C95A] RNase A[e]	3.0 ± 0.2	0.77	3.9 ± 0.2

[a] From ref *12* at pH 6. [b] From the current experiments using the method described in the text. [c] From ref *35* at pH 7. [d] From ref *33* at pH 7. [e] From ref *41* at pH 8.

lacking the analogous (40−95) disulfide bond ([C40A, C95A]) (*39*). The T_m obtained from this method is slightly underestimated compared with other methods, which was also evident when RNase A was used as a test case (*31*).

Midpoint of Chemical Denaturation of Des [30−75]. Figure 1 shows the fraction of des [30−75] ONC and native RNase A as a function of the denaturant concentration. The circles and squares represent des [30−75] ONC and RNase A, respectively. The curves are the fits of sigmoidal functions, from which the midpoints of the denaturing curves were obtained. The GdnHCl denaturing curve and the midpoint of chemical denaturation of RNase A (3.0 M GdnHCl) are consistent with previously reported values using optical techniques under similar conditions (*33*−*35*, *40*). The agreement with these previous results supports the contention that this method provides a reasonable estimate of the chemical denaturing curve. The midpoint of the GdnHCl denaturing curve for des [30−75] ONC is shifted to a lower GdnHCl concentration (2.0 M) compared to that of N-ONC (4.5 M) (*12*), and is therefore indicative of the lower conformational stability of this des species compared to the parent molecule.

The midpoint of the GdnHCl denaturing curve, free energy of unfolding, and the *m* value of des [30−75] ONC at 25 °C are listed in Table 1, which also includes the corresponding values for N-ONC, RNase A, and [C40A, C95A] RNase A from previous reports (*12*, *33*−*35*, *41*). The values of the free energy of unfolding and the *m* values of RNase A obtained from the current experiment are consistent with those from other independent experiments under similar

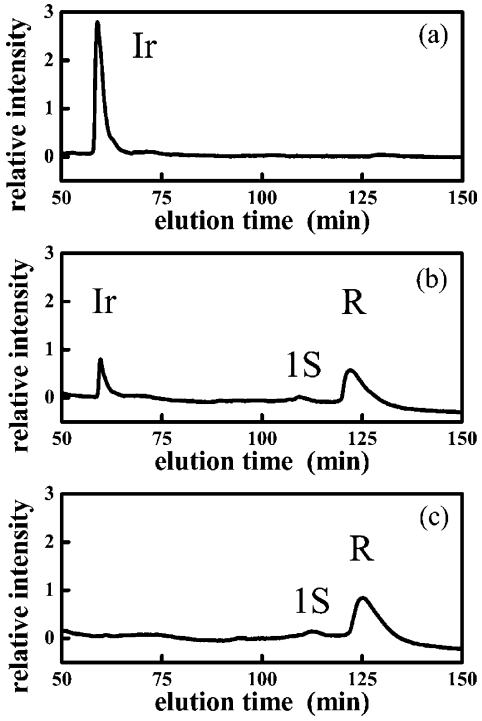

FIGURE 2: HPLC chromatograms showing the reductive unfolding of des [30−75], i.e., the reductive intermediate Ir (*30*), at 0.5 mg/mL protein, 100 mM DTT^{red}, pH 8, and 15 °C, (a) $t = 0$; (b) $t = 30$ h; (c) $t = 120$ h. The small amount of one-disulfide-containing intermediates (1S) may arise from oxidation of R by air and/or DTT^{ox} (which is formed during reductive unfolding).

conditions (*33*, *34*). The ΔG^o_{cu} for des [30−75] ONC is much lower than that of N-ONC, indicating that the stability of the des species is much lower than that of the parent molecule. However, the midpoint and the free energy of unfolding are much larger than those of its homologous mutant [C40A, C95A] RNase A, which indicates that des [30−75] is much more stable than [C40A, C95A] RNase A.

Reductive Unfolding of Des [30−75]. Typical HPLC chromatograms obtained during the reductive unfolding of des [30−75] by DTT^{red} (100 mM, pH 8, and 15 °C) are shown in Figure 2 with the panels a−c representing $t = 0$, 30, and 120 h, respectively. During the reductive unfolding of des [30−75], no intermediate is populated significantly under this experimental condition. The kinetics of the reduction of des [30−75] and the concomitant formation of fully reduced ONC are shown in Figure 3. The two curves in this figure are the fits of single-exponential decay or growth for two species, des [30−75] and reduced ONC (R-ONC), respectively. The time constant for the reduction of des [30−75] under the above experimental condition is about 1600 min (Figure 3).

Kinetic Fate of Des [30−75] ONC. Figure 4 shows the HPLC chromatogram obtained 240 min after the addition of 50 mM DTT^{ox} to des [30−75] in the presence of 0.4 mM DTT^{red} (pH 8, 15 °C). It is evident that there is no other peak present, except at the positions of N-ONC and des [30−75]. The absence of any reduced protein indicates that des [30−75] is oxidized directly to N-ONC (see Discussion). It should be noted that this result alone does not necessarily imply that des [30−75] is significantly populated as an intermediate during the regeneration of fully reduced ONC

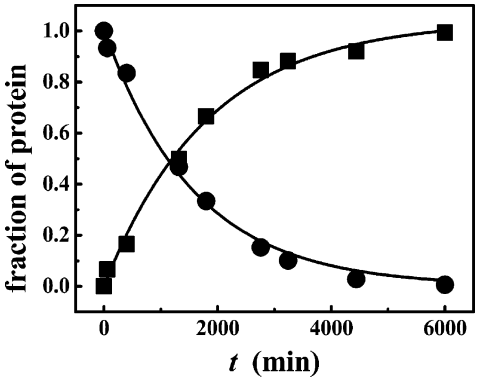

FIGURE 3: Fraction of protein species during the reductive unfolding of des [30−75] at 0.5 mg/mL protein, 100 mM DTT^{red}, pH 8, and 15 °C. The circles and squares represent des [30−75] and R-ONC, respectively. The curves are the fits of single-exponential decay and growth of des [30−75] and R-ONC, respectively.

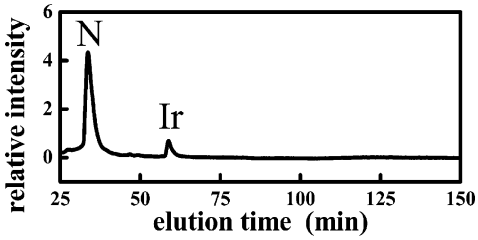

FIGURE 4: HPLC chromatogram showing the oxidation of des [30−75] after a reduction pulse 240 min after introduction of the oxidizing agent. The experimental conditions are 0.5 mg/mL des [30−75] ONC, 50 mM DTT^{ox}, 0.4 mM DTT^{red}, 100 mM Tris-HCl, 1 mM EDTA, pH 8, and 15 °C.

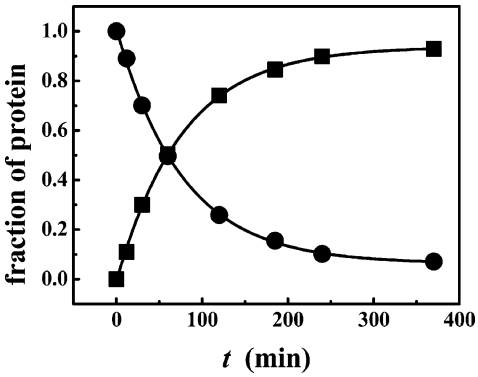

FIGURE 5: Fraction of des [30−75] and native ONC, during the oxidation of des [30−75]. The experimental conditions are those described in the legend to Figure 4. The circles and squares represent des [30−75] and native ONC, respectively. The curves are the fits of single-exponential decay and growth of des [30−75] and native ONC, respectively.

because oxidative folding might proceed through other folding pathway(s).

Figure 5 shows the kinetics of formation of N-ONC and the consumption of des [30−75] during the same experiment as in Figure 4. The time constant for the formation of N-ONC is around 77 min.

Rate of Formation of Structured 3S Species from its 3S Ensembles. The unstructured 3S ensemble was incubated in a pH 8 buffer (100 mM Tris-HCl, 1 mM EDTA) at 25 °C. This condition permits the unstructured intermediates in the 3S ensemble to isomerize by thiol-disulfide reshuffling. The formed structured species are distinguished from the unstructured 3S intermediates by introducing a reduction pulse

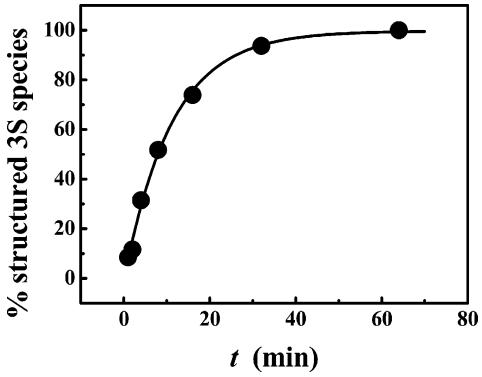

FIGURE 6: Formation of the structured intermediate of ONC from its 3S ensemble. Experimental conditions are 0.5 mg/mL protein, 20 mM Tris-HCl, 1 mM EDTA, pH 8, and 25 °C.

(5 mM DTT^{red}, 2 min) that converts all the unstructured protein to the fully reduced form (R) before blocking the free thiols. Only one peak, in addition to the reduced protein, is detected in the samples after a reduction pulse, indicating the presence of structured species. The peak appears at the same elution time as des [30−75]. The kinetics of formation of the structured 3S species from the unstructured 3S isomers is shown in Figure 6. The curve is a single exponential fit. The 3S ensemble was quantitatively converted to the structured 3S species at the end of the experiment. The rate constant is about 0.09 min^{-1} (or a time constant of ∼11 min) at pH 8 and 25 °C.

Calculation of Entropy of Formation of Three-Disulfide-Bond-Containing Species. To study the bias to form the stable structured intermediates under strongly denaturing conditions, a calculation of the entropy of formation was carried out for all 420 theoretical 3S species. The theoretical abundance of different 3S species is predicted based only on the entropic contributions to the free energy change (*42*). The required entropic changes are calculated by using the following equation (*43*), which is based on a random-flight statistical coil model (*43*−*45*) and on the Wang-Uhlenbeck expression (*46*) for multivariate Gaussian distributions.

$$\Delta S^\circ = R(-3.47n + 3n \ln a - 1.5 \ln |C|) \qquad (3)$$

Here, a is the length of a chain element, n is the number of disulfide bonds, C is a (3 × 3) symmetric matrix whose elements are C_{ij} = (number of residues shared by loops i and j) × (a^2), and $|C|$ is the determinant of C (*43*). If ΔH_i° were the same for all species, the predicted relative abundance [I$_i$] of a given three-disulfide species i from a protein with four disulfides at equilibrium can be calculated by using the entropy change ΔS_i° from eq 4 (*5*), for all 420 possible species.

$$[\mathrm{I}_i] \propto \exp(\Delta S_i^\circ / R) \qquad (4)$$

This method has been applied to the determination of the disulfide-bond distribution of the three-disulfide species of the [C40A, C95A] mutant of RNase A (*7*).

The entropically calculated abundance of different des species of RNase A and ONC is shown in Table 2. None of the des species of RNase A or ONC has a probability of formation larger than 1%.

DISCUSSION

Stability of Des [30−75]. Thermal transition and chemical denaturation data indicate that des [30−75] is conforma-

Table 2: Percentage of Des Species in ONC and RNase A among All 420 3S Species Obtained from a Calculation of Their Entropy of Formation

RNase A	percentage (%)	ONC	percentage (%)
des [26−84]	0.1625	des [19−68]	0.0248
des [40−95]	0.0855	des [30−75]	0.0144
des [58−110]	0.2051	des [48−90]	0.0453
des [65−72]	0.0222	des [87−104]	0.0249

tionally less stable ($\Delta G^{o}_{cu} \sim$ 6.6 kcal/mol) compared to its parent molecule, N-ONC ($\Delta G^{o}_{cu} \sim$ 13.9 kcal/mol), indicating that the (30−75) disulfide bond contributes significantly to the stability of the protein as does the (87−104) disulfide bond (*13*, *15*). Interestingly, the free energy of unfolding of des [30−75] species is closer to that of native RNase A which has four disulfide bonds.

Although our method slightly underestimates the midpoint of the thermal transition, it is extremely useful since it can be applied to determine the thermal transitions of a mixture of structured intermediates that may arise during oxidation regeneration, as long as they can be separated from one another, for example, by HPLC (*31*).

The Disulfide Bonds of Des [30−75] Are Relatively Buried as Compared to the (30−75) Disulfide Bond in N-ONC. In the reductive unfolding of N-ONC, it was demonstrated that the (30−75) bond in N-ONC was easily reducible to form des [30−75] (*30*). The time constant for reductive unfolding of the native protein at 10 mM DTT^{red}, pH 8, and 15 °C is about 43 min (*30*), which is much shorter than about 2300 min [Figure 4a of ref *46*] for the reduction of the first disulfide bond of its homologue, RNase A, at 100 mM DTT^{red}, pH 8, and 15 °C (*46*). The fast, partial reduction of N-ONC compared to RNase A is consistent with a very large exposed surface area of the (30−75) disulfide in N-ONC (*30*).

The time constant for the reductive unfolding of des [30−75] to form fully reduced ONC (100 mM DTT^{red}, 15 °C, pH 8) is ∼1600 min (Figure 3), which is much longer than the 43 min for the reduction of the first disulfide bond of N-ONC at lower DTT^{red} concentration (*30*), and is slightly shorter than the 2300 min for the reduction of the (40−95) and (65−72) disulfide bonds in RNase A under the same condition (100 mM DTT^{red}, pH 8, 15 °C) (*46*). These data indicate that the three disulfide bonds in des [30−75] are relatively inaccessible to the reducing agent as compared to the (30−75) disulfide bond of ONC, but have a relatively similar free energy required for unfolding as the (40−95) and (65−72) disulfide bonds in RNase A (Table 3).

No reductive unfolding intermediate of des [30−75] is observed during its reduction to form fully reduced protein. This is consistent with the absence of any lag time for the formation of R-ONC in Figure 3, while such a lag time is present in the reduction of native ONC (*30*).

To determine the mechanism for the reduction of des [30−75] to form the fully reduced protein (i.e., global vs local unfolding to expose its disulfide bonds), we have calculated the standard free energy of its reduction (*46*). The change in the standard free energy [ΔG^{o}_{ru} (ru: reductive unfolding)] for exposing a disulfide bond for reduction can be obtained from the following relation (*46*).

Table 3: Rate Constants and the Change in Standard Free Energy for Reduction of a Disulfide Bond in Native ONC, Des [30−75] ONC, Wild-Type RNase A, and Its Des Species at 15 °C and pH 8

reduction of proteins	k (min^{-1} M^{-1})	ΔG^{o}_{ru} (kcal mol^{-1})
ONC → des [30−75][a]	2.3 ± 0.2	2.6 ± 0.1
des [30−75] → 2S ONC[b]	(6.3 ± 0.3) × 10^{-3}	6.0 ± 0.1
RNase A → des [40−95][c]	(2.1 ± 0.1) × 10^{-3}	6.6 ± 0.1
RNase A → des [65−72][c]	(2.3 ± 0.1) × 10^{-3}	6.5 ± 0.1
des [40−95] → 2S RNase A[c]	(6.8 ± 0.5) × 10^{-3}	5.9 ± 0.1
des [65−72] → 2S RNase A[c]	(1.8 ± 0.1) × 10^{-3}	6.7 ± 0.1

[a] From the fit of data in ref *30* with 10 mM DTT^{red}. [b] From the fit of the data in the current reduction experiment with 100 mM DTT^{red}. Here, 2S is a group of two-disulfide intermediates formed in the reduction of structured three-disulfide intermediates. The 2S species are not observed in the experiments due to the fast reduction of 2S species under strong reducing conditions because there are no stable structured 2S species in the reductive unfolding of both proteins. [c] From ref *46*.

$$\Delta G^{o}_{ru} = -RT \ln \frac{k}{k_I} \quad (5)$$

Here, k is the experimentally determined rate constant for the reduction of the species of interest, and k_I is the reduction rate constant when the disulfide is totally exposed to the reducing agent. Here, $k_I = 210$ min^{-1} M^{-1} at 15 °C (*46*), obtained from the rate constants for formation and reduction of one- and two-disulfide species measured during the regeneration of RNase A (*19*, *21*). Here, ΔG^{o}_{ru} is different from ΔG^{o}_{cu}, since the latter represents the free energy of global conformational unfolding of the protein, whereas the former could represent the free energy of global or local unfolding of the same multi-disulfide-containing protein. The rate constants for the reduction of the (30−75) disulfide bond in 2S ONC, the reduction of des [30−75] to form R-ONC, and the reduction of the individual disulfide bonds in RNase A (*46*) are shown in Table 3 along with the free energy change for the individual unfolding processes. In Table 3, 2S refers to the three possible native two-disulfide-containing intermediates that can be formed during the reduction of a structured three-disulfide-containing intermediate (i.e., by the reduction of des [30−75] ONC and des [40−95] RNase A). These 2S species are not observed in the experiments due to their fast reduction in the presence of 100 mM DTT^{red}.

The ΔG^{o}_{ru} for the reduction of the (30−75) disulfide bond in ONC is ∼2.6 kcal/mol, which is much smaller than the free energy for conformational unfolding of the native protein ($\Delta G^{o}_{cu} \sim$ 13.9 kcal/mol) at 25 °C (Table 1), indicating that the reduction of this disulfide bond takes place by a local unfolding process. The free energy requirements for the further reduction of des [30−75] to form 2S ONC (which is the rate-determining step in its reduction since the further reduction of 2S to the fully reduced protein is very fast) (∼6.0 kcal/mol at 15 °C) (Table 3) is slightly smaller than the lower limit (*31*) of the free energy for conformational unfolding of the des [30−75] (∼ 6.6 kcal/mol at 25 °C) (Table 1). It should be noted that a global unfolding free energy higher than 6.6 kcal/mol would be expected at lower temperature (15 °C). These results suggest that the reduction of des [30−75] ONC occurs through a local unfolding step. The reduction rate constant of des [30−75] [(6.3 ± 0.3) × 10^{-3} min^{-1} M^{-1}] is comparable to that of the analogous

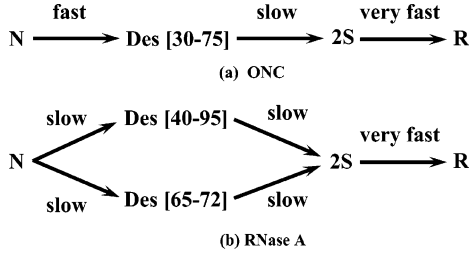

FIGURE 7: Reductive unfolding pathway(s) of (a) ONC and (b) RNase A at pH 8 and 15 °C.

intermediate of RNase A, des [40−95] [$(6.8 \pm 0.5) \times 10^{-3}$ min^{-1} M^{-1}] (Table 3), although des [30−75] ONC is much more stable than des [40−95] RNase A based on a comparison of the free energies of conformational unfolding (global unfolding) of the two proteins at 25 °C [ΔG^{o}_{cu} is 6.6 and 3.0 kcal/mol for des [30−75] and [C40A, C95A] RNase A, respectively (Table 1)].

From the previous studies of the partial reduction of ONC (*30*) and the reduction of des [30−75] ONC reported here, the reduction pathway of ONC can be described by the scheme of Figure 7a. The 2S species are not observed in the experiments due to the fast reduction of 2S species under strong reducing conditions. The reduction of the frog ribonuclease takes place by a single pathway involving the fast formation of des [30−75]. By contrast, the bovine variant undergoes reductive unfolding through two parallel pathways to form two structured intermediates, des [40−95] and des [65−72] (Figure 7b) (*46*). The origin of this dissimilarity of the two pathways has been discussed in detail elsewhere (*30*).

Kinetic Properties of Des [30−75]. The isolation of unblocked des [30−75] makes it possible to study two key elementary steps in the oxidative folding of ONC and their comparison with the analogous processes in its homologue, RNase A. First, since the major oxidative folding intermediate of RNase A, des [40−95] (analogous to des [30−75] ONC) is a disulfide-secure species (*36*), it was possible to determine whether des [30−75] is a disulfide-secure species or not. We define disulfide-secure species (e.g., des [65−72] and des [40−95] in RNase A) as those that keep their disulfide bonds buried, and expose their thiols (if not already exposed) by a local unfolding mechanism which enables their oxidation to form the native protein; we define disulfide-insecure species, (e.g., des [58−110] and des [26−84] in RNase A) as those that have their free thiols buried and need global unfolding to expose them for oxidation. The global unfolding of the protein invites a competition between intramolecular thiol-disulfide reshuffling and the two-step oxidation process, which results in a majority of the disulfide-insecure intermediate being reshuffled back to its unstructured isomers (*36*, *47*). This also occurred in the oxidation step from unstructured 3S species to native protein during the regeneration on a des pathway (*36*). Second, the rate-determining step in oxidative folding of RNase A is the formation of the structured des species from the unstructured 3S ensemble through reshuffling reactions. Now, it is possible to compare this process to the analogous steps in ONC (see the last paragraph of the Discussion).

Des [30−75] Is a Disulfide-Secure Intermediate. Data on the oxidation of des [30−75] to N-ONC (Figures 4 and 5) indicate the quantitative formation of the native molecule from its reductive intermediate in the presence of a small amount of reducing agent (0.4 mM DTT^{red}) that was added to the oxidizing buffer (50 mM DTT^{ox}, 100 mM Tris-HCl, 1 mM EDTA, pH 8, 15 °C). While the small amount of reducing agent is sufficient to reduce any unstructured species to R-ONC, any structured intermediate that is present (such as des [30−75]) is unaffected. The absence of any fully reduced ONC indicates the *direct* formation of N-ONC from des [30−75] since it excludes the presence of any unstructured 3S isomers which would be populated in an *indirect* oxidation process and would have been reduced to R-ONC under conditions used here. These data prove that des [30−75] is a disulfide-secure intermediate which is not kinetically trapped under the given conditions.

In oxidative folding of ONC, two peaks in the cation-exchange chromatogram (obtained using a Rainin Hydropore 5-SCX column) were identified as containing structured 3S species (unpublished results). The elution time of one of these peaks agrees well with that of des [30−75]. Nevertheless, it remains to be seen whether this intermediate is significantly populated along the oxidative folding pathway of ONC.

The Propensity to Form Structured Species from Unstructured 3S Ensembles. The formation of des species was initiated by the reshuffling of the unstructured 3S ensemble. Figure 6 shows the percentage of the only peak containing at least one structured species, which is present after a reduction pulse, as a function of incubation time. The elution time of this peak in the ONC chromatogram agrees well with that of des [30−75]. However, since other des species may elute at the same time, the identity of the structured species cannot be determined with certainty from the present data. Future disulfide mapping data will enable us to determine the species present at the end of the isomerization process. The structured intermediate species of ONC forms faster from its unstructured 3S ensemble by reshuffling than does the des species of RNase A in the analogous process [the rate constants for the formation of the structured species are 0.09 and 0.014 min^{-1} for structured 3S ONC and des [40−95] RNase A (*23*), respectively, under the same conditions]. A calculation of the entropy of formation of 3S species of ONC and RNase A indicates that, while none of the des species in either variant has a probability of formation greater than 1%, the origin of this difference is not the result of the difference in the disulfide bond pattern of the two proteins since almost all the des species of RNase A have larger abundance than those of ONC (Table 2). Three possible reasons may account for this result: (i) Some enthalpic interactions, which favor the native disulfide bonds over non-native ones to a much greater extent in ONC than in RNase A, may exist in the unstructured species of ONC. (ii) It was hypothesized that the conformational folding rate of a structured disulfide intermediate has a profound effect on the overall regeneration rates (*48*). Therefore, another possible reason is that the conformational folding rate of ONC is much faster than that of RNase A. (iii) It is also possible that ONC has some much more reactive thiols than RNase A that accelerate the reshuffling process. Further research is needed to distinguish between these possibilities and to characterize the underlying interactions.

CONCLUSION

We have characterized des [30−75], a fast-forming intermediate in the reductive unfolding of ONC. Our data

indicate that the (30−75) disulfide bond in ONC contributes significantly to the stability of the protein. Further reduction of des [30−75] is a slow process that requires at least partial unfolding of the intermediate to expose the remaining disulfides to the reducing agent. No further reductive intermediates of des [30−75] accumulate before the formation of the fully reduced protein.

Furthermore, similar to the analogous des [40−95] intermediate of the homologue RNase A, des [30−75] is a disulfide-secure productive intermediate that would be a critical asset in the oxidative folding of ONC. Des [30−75] might be significantly populated in the oxidative regeneration pathway. The formation of the structured des species from the unstructured isomers is faster than that of des [40−95] RNase A.

ACKNOWLEDGMENT

The authors appreciate the help provided by Laura Hathaway and Celestine Wanjalla during the expression of ONC.

REFERENCES

1. Ardelt, W., Mikulski, S. M., and Shogen, K. (1991) Amino acid sequence of an anti-tumor protein from *Rena pipiens* oocytes and early embryos. Homology to pancreatic ribonucleases. *J. Biol. Chem. 266*, 245−251.
2. Mosimann, S. C., Ardelt, W., and James, M. N. (1994) Refined 1.7 Å X-ray crystallographic structure of P-30 protein, an amphibian ribonuclease with anti-tumor activity. *J. Mol. Biol. 236*, 1141−1153.
3. Altmann, K. H., and Scheraga, H. A. (1990) Local structure in ribonuclease A. Effect of amino acid substitutions on the preferential formation of the native disulfide loop in synthetic peptides corresponding to residues Cys^{58}-Cys^{72} of bovine pancreatic ribonuclease A. *J. Am. Chem. Soc. 112*, 4926−4931.
4. Xu, X., Rothwarf, D. M., and Scheraga, H. A. (1996) Nonrandom distribution of the one-disulfide intermediates in the regeneration of ribonuclease A. *Biochemistry 35*, 6406−6417.
5. Volles, M. J., Xu, X., and Scheraga, H. A. (1999) Distribution of disulfide bonds in the two-disulfide intermediates in the regeneration of bovine pancreatic ribonuclease A: Further insights into the folding process. *Biochemistry 38*, 7284−7293.
6. Carty, R. P., Pincus, M. R., and Scheraga, H. A. (2002) Interactions that favor the native over the non-native disulfide bond among residues 58−72 in the oxidative folding of bovine pancreatic ribonuclease A. *Biochemistry 41*, 14815−14819.
7. Wedemeyer, W. J., Xu, X., Welker E., and Scheraga, H. A. (2002) Conformational propensities of protein folding intermediates: Distribution of species in the 1S, 2S, and 3S ensembles of the [C40A, C95A] mutant of bovine pancreatic ribonuclease A. *Biochemistry 41*, 1483−1491.
8. Harrington, W. F., and Schellman, J. A. (1956) Evidence for the instability of hydrogen-bonded peptide structures in water, based on studies of ribonuclease and oxidized ribonuclease. *C. R. Trav. Lab. Carlsberg Chim. 30*, 21−43.
9. Hermans, J. Jr., and Scheraga, H. A. (1961) Structural studies of ribonuclease. V. Reversible change of configuration. *J. Am. Chem. Soc. 83*, 3283−3292.
10. Boix, E., Wu, Y.-N., Vasandani, V. M., Saxena, S. K., Ardelt, W., Ladner, J., and Youle, R. J. (1996) Role of the N terminus in RNase A homologues: Differences in catalytic activity, ribonuclease inhibitor interaction and cytotoxicity. *J. Mol. Biol. 257*, 992−1007.
11. Leland, P. A., Schultz, L. W., Kim, B.-M., and Raines, R. T. (1998) Ribonuclease A variants with potent cytotoxic activity. *Proc. Natl. Acad. Sci. U.S.A. 95*, 10407−10412.
12. Notomista, E., Catanzano, F., Graziano, G., Dal Piaz, F., Barone, G., D'Alessio, G., and Di Donato, A. (2000) Onconase: an unusually stable protein. *Biochemistry 39*, 8711−8718.
13. Notomista, E., Catanzano, F., Graziano, G., Di Gaetano, S., Barone, G., and Di Donato, A. (2001) Contribution of chain termini to the conformational stability and biological activity of onconase. *Biochemistry 40*, 9097−9103.
14. Newton, D. L., Boque, L., Wlodawer, A., Huang, C. Y., and Rybak, S. M. (1998) Single amino acid substitutions at the N-terminus of a recombinant cytotoxic ribonuclease markedly influence biochemical and biological properties. *Biochemistry 37*, 5173−5183.
15. Leland, P. A., Staniszewski, K. E., Kim, B.-M., and Raines, R. T. (2000) A synapomorphic disulfide bond is critical for the conformational stability and cytotoxicity of an amphibian ribonuclease. *FEBS Lett. 477*, 203−207.
16. Mendoza, J. A., Jarstfer, M. B., and Goldenberg, D. P. (1994) Effects of amino acid replacements on the reductive unfolding kinetics of pancreatic trypsin inhibitor. *Biochemistry 33*, 1143−1148.
17. Vasandani, V. M., Wu, Y. N., Mikulski, S. M., Youle, R. J., and Sung, C. (1996) Molecular determinants in the plasma clearance and tissue distribution of ribonucleases of the ribonuclease A superfamily. *Cancer Res. 56*, 4180−4186.
18. Rothwarf, D. M., and Scheraga, H. A. (1993) Regeneration of bovine pancreatic ribonuclease A. 1. Steady-state distribution. *Biochemistry 32*, 2671−2679.
19. Rothwarf, D. M., and Scheraga, H. A. (1993) Regeneration of bovine pancreatic ribonuclease A. 2. Kinetics of regeneration. *Biochemistry 32*, 2680−2689.
20. Rothwarf, D. M., and Scheraga, H. A. (1993) Regeneration of bovine pancreatic ribonuclease A. 3. Dependence on the nature of the redox reagent. *Biochemistry 32*, 2690−2697.
21. Rothwarf, D. M., and Scheraga, H. A. (1993) Regeneration of bovine pancreatic ribonuclease A. 4. Temperature dependence of the regeneration rate. *Biochemistry 32*, 2698−2703.
22. Rothwarf, D. M., Li, Y.-J., and Scheraga, H. A. (1998) Regeneration of bovine pancreatic ribonuclease A: Identification of two nativelike three-disulfide intermediates involved in separate pathways. *Biochemistry 37*, 3760−3766.
23. Rothwarf, D. M., Li, Y.-J., and Scheraga, H. A. (1998) Regeneration of bovine pancreatic ribonuclease A: Detailed kinetic analysis of two independent folding pathways. *Biochemistry 37*, 3767−3776.
24. Welker, E., Narayan, M., Volles, M. J., and Scheraga, H. A. (1999) Two new structured intermediates in the oxidative folding of RNase A. *FEBS Lett. 460*, 477−479.
25. Goldenberg, D. P. (1988) Kinetic analysis of the folding and unfolding of a mutant form of bovine pancreatic trypsin inhibitor lacking the cysteine-14 and -38 thiols. *Biochemistry 27*, 2481−2489.
26. Kuwajima, K., Ikeguchi, M., Sugawara, T., Hiraoka, Y., and Sugai, S. (1990) Kinetics of disulfide bond reduction in α-lactalbumin by dithiothreitol and molecular basis of superreactivity of the Cys6-Cys120 disulfide bond. *Biochemistry 29*, 8240−8249.
27. Ewbank, J. J., and Creighton, T. E. (1993) Pathway of disulfide-coupled unfolding and refolding of bovine α-lactalbumin. *Biochemistry 32*, 3677−3693.
28. Ma, L.-C., and Anderson, S. (1997) Correlation between disulfide reduction and conformational unfolding in bovine pancreatic trypsin inhibitor. *Biochemistry 36*, 3728−3736.
29. Chang, J.-Y. (1997) A two-stage mechanism for the reductive unfolding of disulfide-containing proteins. *J. Biol. Chem. 272*, 69−75.
30. Narayan, M., Xu, G., Ripoll, D. R., Zhai, H., Breuker, K., Leung, H. J., Wanjalla, C., Navon, A., Welker, E., McLafferty, F. W., and Scheraga, H. A. Dissimilarity in the reductive unfolding pathways of two ribonuclease homologues. *J. Mol. Biol.*, manuscript submitted.
31. Xu, G., Narayan, M., Welker, E., and Scheraga, H. A. (2003) A novel method to determine thermal transition curves of disulfide-containing proteins and their structured folding intermediates. *Biochem. Biophys. Res. Comm. 311*, 514−517.
32. Santoro, M. M., and Bolen, D. W. (1988) Unfolding free energy changes determined by the linear extrapolation method. 1. Unfolding of phenylmethanesulfonyl α-chymotrypsin using different denaturants. *Biochemistry 27*, 8063−8068.
33. Pace, C. N. (1990) Measuring and increasing protein stability. *Trends Biotechnol. 8*, 93−98.
34. Pace, C. N., Laurents, D. V., and Thomson, J. A. (1990) pH dependence of the urea and guanidine hydrochloride denaturation of ribonuclease A and ribonuclease T1. *Biochemistry 29*, 2564−2572.

35. Ahmad, F., Yadav, S., and Taneja, S. (1992) Determining stability of proteins from guanidinium chloride transition curves. *Biochem. J. 287*, 481−485.
36. Welker, E., Narayan, M., Wedemeyer, W. J., and Scheraga, H. A. (2001) Structural determinants of oxidative folding in proteins. *Proc. Natl. Acad. Sci. U.S.A. 98*, 2312−2316.
37. Tsong, T. Y., Hearn, R. P., Wrathall, D. P., and Sturtevant, J. M. (1970) A calorimetric study of thermally induced conformational transitions of ribonuclease A and certain of its derivatives. *Biochemistry 9*, 2666−2677.
38. Pace, C. N., Grimsley, G. R., Thomas, S. T., and Makhatadze, G. I. (1999) Heat capacity change for ribonuclease A folding. *Protein Sci. 8*, 1500−1504.
39. Laity, J. H., Lester, C. C., Shimotakahara, S., Zimmerman, D. E., Montelione, G. T., and Scheraga, H. A. (1997) Structural characterization of an analogue of the major rate-determining disulfide folding intermediate of bovine pancreatic ribonuclease A. *Biochemistry 36*, 12683−12699.
40. Ahmad, F., and Bigelow, C. C. (1982) Estimation of the free energy of stabilization of ribonuclease A, lysozyme, α-lactalbumin, and myoglobin. *J. Biol. Chem. 257*, 12935−12938.
41. Iwaoka, M., Wedemeyer, W. J., and Scheraga, H. A. (1999) Conformational unfolding studies of three-disulfide mutants of bovine pancreatic ribonuclease A and the coupling of proline isomerization to disulfide redox reactions. *Biochemistry 38*, 2805−2815.
42. Lin, S. H., Konishi, Y., Denton, M. E., and Scheraga, H. A. (1984) Influence of an extrinsic cross-link on the folding pathway of ribonuclease A. Conformational and thermodynamic analysis of cross-linked (lysine^{7}- lysine^{41})-ribonuclease A. *Biochemistry 23*, 5504−5512.
43. Flory, P. J. (1953) *Principles of Polymer Chemistry*, Chapter X, Cornell University Press, Ithaca, NY.
44. Poland, D. C., and Scheraga, H. A. (1965) Statistical mechanics of noncovalent bonds in polyamino acids. 8. Covalent loops in proteins. *Biopolymers 3*, 379−399.
45. Wang, M. C., and Uhlenbeck, G. F. (1945) On the theory of the Brownian motion II. *Rev. Mod. Phys. 17*, 323−342.
46. Li, Y.-J., Rothwarf, D. M., and Scheraga, H. A. (1995) Mechanism of reductive protein unfolding. *Nat. Struct. Biol. 2*, 489−494.
47. Narayan, M., Welker, E., Wanjalla, C., Xu, G., and Scheraga, H. A. (2003) Shifting the competition between the intramolecular Reshuffling reaction and the direct oxidation reaction during the oxidative folding of kinetically trapped disulfide-insecure intermediates. *Biochemistry 42*, 10783−10789.
48. Welker, E., Wedemeyer, W. J., Narayan, M., and Scheraga, H. A. (2001) Coupling of conformational folding and disulfide-bond reactions in oxidative folding of proteins. *Biochemistry 40*, 9059−9064.

BI036215D